

The Structure and Evolution of Young Stellar Clusters

Lori Allen, S. Thomas Megeath, Robert Gutermuth

Harvard-Smithsonian Center for Astrophysics

Philip C. Myers, Scott Wolk

Harvard-Smithsonian Center for Astrophysics

Fred C. Adams

University of Michigan

James Muzerolle, Erick Young

University of Arizona

Judith L. Pipher

University of Rochester

We examine the properties of embedded clusters within 1 kiloparsec using new data from the *Spitzer Space Telescope*, as well as recent results from 2MASS and other ground-based near-infrared surveys. We use surveys of entire molecular clouds to understand the range and distribution of cluster membership, size and surface density. The *Spitzer* data demonstrate clearly that there is a continuum of star-forming environments, from relative isolation to dense clusters. The number of members of a cluster is correlated with the cluster radius, such that the average surface density of clusters having a few to a thousand members varies by a factor of only a few. The spatial distributions of *Spitzer*-identified young stellar objects frequently show elongation, low density halos, and sub-clustering. The spatial distributions of protostars resemble the distribution of dense molecular gas, suggesting that their morphologies result directly from the fragmentation of the natal gas. We also examine the effects of the cluster environments on star and planet formation. Although Far-UV and Extreme-UV radiation from massive stars can truncate disks in a few million years, fewer than half of the young stars in our sample (embedded clusters within 1 kpc) are found in regions of strong FUV and EUV fields. Typical volume densities and lifetimes of the observed clusters suggest that dynamical interactions are not an important mechanism for truncating disks on solar system size scales.

1. INTRODUCTION

Since PP IV, there have been significant advances in observations of young stellar clusters from X-ray to millimeter wavelengths. But while much of the recent work has concentrated on the stellar initial mass function (IMF) or protoplanetary disk evolution (e.g., *Lada and Lada, 2003*), less attention has been directed to discerning the structure of young embedded clusters, and the evolution of that structure during the first few million years. Physical properties of young embedded clusters, such as their shapes, sizes, and densities, should inform theories of cluster formation. In this contribution, we describe recent results in which these properties are obtained for a representative sample of young (1-3 Myr), nearby ($d \leq 1$ kpc), embedded clusters.

This contribution is motivated by three recent surveys made with the *Spitzer Space Telescope*: the *Spitzer* Young Stellar Cluster Survey – which includes *Spitzer*, near-IR, and millimeter-wave images of 30 clusters, the *Spitzer* Orion Molecular Cloud Survey – which covers 6.8 sq.

degrees in Orion, and the Cores to Disks (c2d) Legacy program, which surveyed several nearby molecular clouds (*Evans et al., 2003*). These surveys provide a comprehensive census of nearly all the known embedded clusters in the nearest kiloparsec, ranging from small groups of several stars to rich clusters with several hundred stars. A new archival survey from *Chandra* (ANCHORS) is providing X-ray data for many of the nearby clusters. Since PP IV, the *Two Micron All Sky Survey* (2MASS) has become widely used as an effective tool for mapping large regions of star formation, particularly in the nearby molecular clouds. This combination of X-ray, near-IR and mid-IR data is a powerful means for studying embedded populations of pre-main sequence stars and protostars.

Any study of embedded clusters requires some method of identifying cluster members, and we begin by briefly reviewing methods which have progressed rapidly since PP IV, including work from X-ray to submillimeter wavelengths, but with an emphasis on the mid-infrared spectrum

covered by *Spitzer*. Beyond Section 2 we focus almost entirely on recent results from *Spitzer*, rather than a review of the literature. In Section 3, we discuss the cluster properties derived from large-scale surveys of young embedded clusters in nearby molecular clouds, including their sizes, spatial distributions, surface densities, and morphologies. In Section 4 we consider the evolution of young embedded clusters as the surrounding molecular gas begins to disperse. In Section 5 we discuss theories of embedded cluster evolution, and in Section 6 consider the impact of the cluster environment on star and planet formation. Our conclusions are presented in Section 7.

2. METHODS OF IDENTIFYING YOUNG STARS IN CLUSTERS

2.1. Near- and Mid-infrared

Young stellar objects (YSOs) can be identified and classified on the basis of their mid-infrared properties (Adams *et al.*, 1987; Wilking *et al.*, 1989; Myers and Ladd, 1993). Here we review recent work on cluster identification and characterization based primarily on data from the *Spitzer* Space Telescope.

Megeath *et al.* (2004) and Allen *et al.* (2004) developed YSO classification schemes based on color-color diagrams from observations taken with the Infrared Array Camera (IRAC) on *Spitzer*. Examining models of protostellar envelopes and circumstellar disks with a wide range of plausible parameters, they found that the two types of objects should occupy relatively distinct regions of the diagram. Almost all of the Class I (star+disk+envelope) models exhibited the reddest colors, not surprisingly, with the envelope density and central source luminosity having the most significant effect on the range of colors. The Class II (star+disk) models included a treatment of the inner disk wall at the dust sublimation radius, which is a significant contributor to the flux in the IRAC bands. Models of the two classes generally occupy distinct regions in color space, indicating that they can be identified fairly accurately from IRAC data even in the absence of other information such as spectra.

Comparison of these loci with YSOs of known types in the Taurus star forming region shows reasonably good agreement (Hartmann *et al.*, 2005). Some degeneracy in the IRAC color space does exist; Class I sources with low envelope column densities, low mass infall rates or certain orientations may have the colors of Class II objects. The most significant source of degeneracy is from extreme reddening due to high extinction, which can cause Class II objects to appear as low-luminosity Class I objects when considering wavelengths $\lambda \lesssim 10 \mu\text{m}$.

The addition of data from the $24 \mu\text{m}$ channel of the Multiband Imaging Photometer for *Spitzer* (MIPS) provides a longer wavelength baseline for classification, particularly useful for resolving reddening degeneracy between Class I and II. It is also crucial for robust identification of evolved disks, both “transition” and “debris”, which lack excess

emission at shorter wavelengths due to the absence of dust close to the star. Such $24 \mu\text{m}$ observations are limited, however, by lower sensitivity and spatial resolution compared to IRAC, as well as the generally higher background emission seen in most embedded regions. Muzerolle *et al.* (2004) delineated Class I and II loci in an IRAC/MIPS color-color diagram of one young cluster based on the $3.6\text{--}24 \mu\text{m}$ spectral slope.

The choice of classification method depends partly on the available data; not all sources are detected (or observed) in the 2MASS, IRAC, and MIPS bands. IRAC itself is significantly more sensitive at 3.5 and $4.5 \mu\text{m}$ than at 5.8 and $8 \mu\text{m}$, so many sources may have IRAC detections in only the two shorter wavelengths, and require a detection in one or more near-IR bands to classify young stars (Gutermuth *et al.*, 2004; Megeath *et al.*, 2005; Allen *et al.*, 2005). Gutermuth *et al.* (2006) refined the IRAC+near-IR approach by correcting for the effects of extinction, estimated from the $H - K$ color, and developed new classification criteria based on the extinction-corrected colors.

It is useful to compare some of the different classification schemes. In Fig. 1 we plot first a comparison of the IRAC model colors from Allen *et al.* (2004), Hartmann *et al.* (2005) and Whitney *et al.* (2003). In general, the models predict a similar range of IRAC colors for both Class I and Class II sources. Also in Fig. 1 we plot the same sample of IRAC data (NGC 2068/71) from Muzerolle *et al.* (2006) in three color-color planes which correspond to the classification methods discussed above. In all diagrams, only those sources with detections in the three 2MASS bands, the four IRAC bands, and the MIPS $24 \mu\text{m}$ band were included. For the sake of comparison with pre-*Spitzer* work, the points are coded according to their $K\text{--}24\mu\text{m}$ SED slope. Prior to *Spitzer*, a commonly used 4-class system was determined by the $2\text{--}10 \mu\text{m}$ (or $2\text{--}20 \mu\text{m}$) slope (α), in which $\alpha > 0.3$ = Class I, $-0.3 \leq \alpha < 0.3$ = “flat” spectrum, $-1.6 \leq \alpha < -0.3$ = Class II, and $\alpha < -1.6$ = Class III (photosphere) (Greene *et al.*, 1994). A few of the sources in Fig. 1 have been observed spectroscopically and determined to be T-Tauri stars, background giants, or dwarfs unassociated with the cluster. These are indicated. The diagrams also show the adopted regions of color space used to roughly distinguish between Class I and Class II objects.

Classifications made with these methods are in general agreement with each other, though some differences are apparent. For example, roughly 30% of Class I objects identified with the Allen *et al.* method and detected at $24 \mu\text{m}$ appear as Class II objects in the IRAC/MIPS- $24 \mu\text{m}$ color space, however many of these are borderline “flat spectrum” sources where the separation between Class I and II is somewhat arbitrary and may not be physically meaningful.

These classification methods implicitly assume that all objects that exhibit infrared excess are YSOs. However, there can be contamination from other sources, including evolved stars, AGN, quasars, and high-redshift dusty galaxies. Since most of these unrelated objects are faint high-redshift AGN (Stern *et al.*, 2005), we have found that a

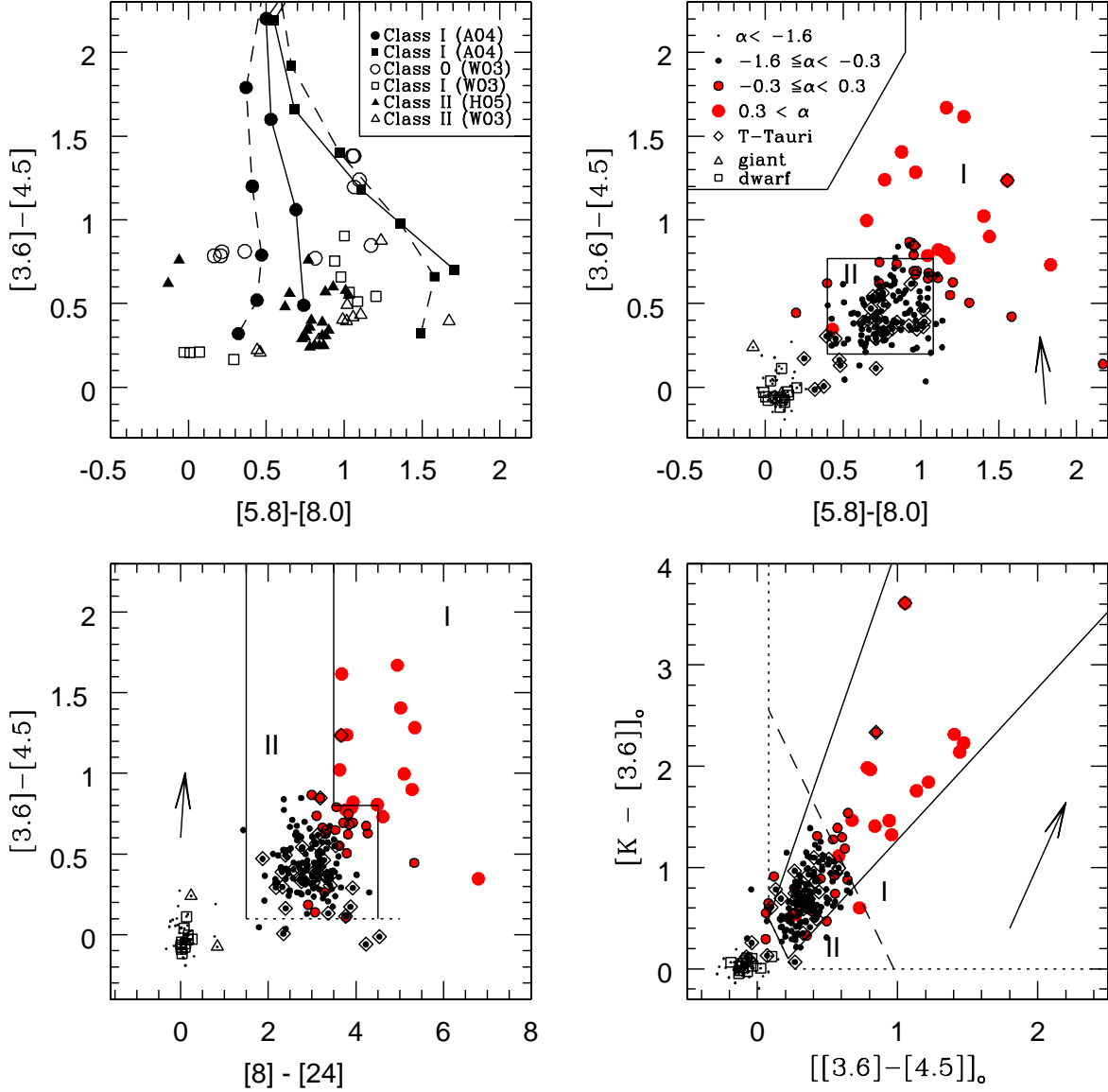


Fig. 1.— Identifying and classifying young stars using near- and mid-infrared measurements. In the panel at top left, a comparison of predicted IRAC colors from *Allen et al.* (2004) (A04), *Hartmann et al.*, (2005) (H05) and *Whitney et al.*, (2003) (W03). Triangles represent Class II models with $T_{\text{eff}} = 4000\text{K}$ and a range of accretion rates, grain size distributions, and inclinations. Squares and circles are Class I/0 models for a range of envelope density, centrifugal radius, and central source luminosity. In the remaining panels, we plot the data for the embedded cluster NGC2068/71 (*Muzerolle et al.*, 2006). Point types are coded according to the measured SED slope between 2 and 24 μm . Spectroscopically confirmed T-Tauri, giant, and dwarf stars are indicated. In the top right panel, the large rectangle marks the adopted domain of Class II sources; the Class I domain is above and to the right (adapted from *Allen et al.*, 2004). In the bottom right panel (*Gutermuth et al.*, 2006), dereddened colors are separated into Class I and II domains by the dashed line. Diagonal lines outline the region where most of the classifiable sources are found. In the bottom left panel, the approximate domains of Class I and II sources are indicated by the solid lines. The dotted line represents the adopted threshold for excess emission at 3.6 and 4.5 μm ; sources below this that exhibit large $[8] - [24]$ excess are probably disks with large optically thin or evacuated holes (adapted from *Muzerolle et al.*, 2004). Arrows show extinction vectors for $A_V = 30$ (*Flaherty et al.*, 2006). These figures show that the various color planes considered here yield similar results when used to classify *Spitzer* sources.

magnitude cut of $m_{3.6} < 14$ will remove all but approximately 10 non-YSOs per square degree within each of the IRAC-only Class I and Class II loci, and all but a few non-YSOs per square degree from the IRAC/MIPS-24 loci, while retaining most if not all of the cluster population.

2.2. Submillimeter and Millimeter

The youngest sources in star forming regions are characterized by strong emission in the sub-millimeter and far-infrared, but usually weak emission shortward of $24 \mu\text{m}$. These “Class 0” objects were first discovered in sub-mm surveys of molecular clouds (André *et al.*, 1993). They are defined as protostars with half or more of their mass still in their envelopes, and emitting at least 0.5% of their luminosity at submillimeter wavelengths. Motivated in part by the discovery of Class 0 objects, observers have imaged many embedded clusters in their dust continuum emission at millimeter and submillimeter wavelengths, revealing complex filamentary structure and many previously unknown sources (e.g., Nutter *et al.*, 2005; Sandell and Knee, 2001; Motte *et al.*, 2001, 1998).

These submillimeter and millimeter wavelength images generally have tens to hundreds of local maxima, but only a small fraction of these are “protostars” having an internal heating source; the rest are “starless cores” having a maximum of column density but no internal heating source. The standard way to determine whether a submm source is a protostar or a starless core is to search for coincidence with an infrared point source, such as a *Spitzer* source at 24 or $70 \mu\text{m}$, or a radio continuum point source, such as a VLA source at 6 cm wavelength. For example the protostars NGC1333-IRAS 4A, 4B, and 4C in Fig. 2 are each detected at $850 \mu\text{m}$ (Sandell and Knee, 2001), and each has a counterpart in VLA observations (Rodriguez *et al.*, 1999) and in $24 \mu\text{m}$ *Spitzer* observations, but not in the IRAC bands. In a few cases, Class 0 protostars such as VLA1623 have been identified from their submm emission and their radio continuum, but not from their mid-infrared emission, because their mid-infrared emission is too heavily extinguished (André *et al.*, 2000).

2.3. X-ray

Elevated X-ray emission is another signature of youth: young stellar objects have typical X-ray luminosity 1000 times that of the Sun. The e-folding decay time for this X-ray luminosity is a few 100 million years (see e.g., Micela *et al.*, 1985; Walter and Barry, 1991; Dorren *et al.*, 1995; Feigelson and Montmerle, 1999). Although the X-ray data of young stellar clusters will be contaminated by AGN and other sources, this contamination can be reduced by identifying optical/infrared counterparts to the X-ray sources. X-ray sources where the ratio of the X-ray luminosity to the bolometric luminosity (L_X/L_{bol}) ranges from 0.1% to 0.01% are likely pre-main sequence stars. In contrast to the infrared techniques described in 2.1, which can only identify Class 0/I and II sources; X-ray observations can readily

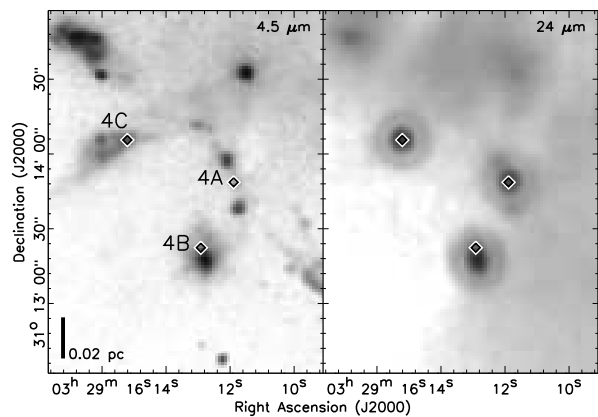


Fig. 2.— IRAC $4.5 \mu\text{m}$ and MIPS $24 \mu\text{m}$ images of IRAS-4 in NGC 1333. MIPS detects each of the three VLA sources, while IRAC detects their outflows but not the driving sources.

detect class II and class III objects, with perhaps some bias toward class III objects (Flacomio *et al.*, 2003). The main limitation of X-ray observations is the lack of sensitivity toward lower mass stars. A complete sample of stars requires a sensitivity toward sources with luminosities as low as $10^{27} \text{ erg cm}^{-2} \text{ s}^{-1}$ (Feigelson *et al.*, 2005), the sensitivity of most existing observations are an order of magnitude higher. The observed X-ray luminosity is also affected by extinction. Depending on the energy of the source, the sensitivity can be reduced by a factor of ten for sources at $A_V \sim 10$ (Wolk *et al.*, 2006).

2.4. Emission Lines and Variability

Among other techniques for identifying young cluster members, spectroscopic surveys for emission lines and photometric surveys for variability have been used successfully at visible and near-IR wavelengths. The most common means of identifying young stars spectroscopically is through detection of optical emission lines, in particular $H\alpha$ at 6563 \AA (Herbig and Bell, 1988). Large-scale objective prism (Wiramihardja *et al.*, 1989; Wilking *et al.*, 1987) and later, wide-field multi-object spectroscopy (e.g., Hillenbrand *et al.*, 1993) has been effective in identifying young stars in clusters and throughout molecular clouds, however they miss the deeply embedded members that are optically faint or invisible. This problem is partly alleviated by large-scale surveys for photometric variability in the optical and near-IR. Recent near-IR surveys by Kaas (1999) and Carpenter *et al.* (2001, 2002) have been successful at identifying young cluster members in Serpens, Orion and Chamaeleon, respectively.

2.5. Star Counts

Much of the work on the density, size, and structure of embedded clusters has relied on using star counts; indeed, the distribution of $2.2 \mu\text{m}$ sources were used to iden-

tify clusters in the Orion B cloud in the seminal work of *Lada et al.* (1991). Instead of identifying individual stars as members, methods based on star counts include all detected sources and employ a statistical approach toward membership, in which an average density of background stars is typically estimated and subtracted out. In this analysis, the star counts are typically smoothed to produce surface density maps; a variety of smoothing algorithms are in the literature (*Gomez et al.*, 1993; *Gladwin et al.*, 1999; *Carpenter*, 2000; *Gutermuth et al.*, 2005; *Cambresy et al.*, 2006).

The degree of contamination by foreground and background stars is the most significant limitation for star count methods, and the efficacy of using star counts depends strongly on the surface density of contaminating stars. In many cases, the contamination can be minimized by setting a K -band brightness limit (*Gutermuth*, 2005; *Lada et al.*, 1991). To estimate the position dependent contamination by field stars, models or measurements of the field star density can be combined with extinction maps of the molecular cloud (*Carpenter*, 2000; *Gutermuth et al.*, 2005; *Cambresy*, 2006). These maps are subtracted from the surface density of observed sources to produce maps of the distribution of embedded stars; however, these maps are still limited by the remaining Poisson noise from the subtracted stars.

Star count methods have the advantage that they do not discriminate against sources without infrared excess, bright X-ray emission, variability, or some other indication of youth. On the other hand, they only work in regions where the surface density of member stars is higher than the statistical noise from contaminating field stars. In Fig. 3 we show maps of the IRAS 20050 cluster derived from the K -band star counts and from the distribution of infrared-excess sources. In the case of IRAS 20050, we find that the star count method provides a better map of the densest regions (due in part to confusion with bright nebosity and sources in the *Spitzer* data), while the lower density regions surrounding these peaks are seen only in the distribution of *Spitzer* identified infrared excess sources (due to the high density of background stars).

3. THE STRUCTURE AND EVOLUTION OF CLUSTERS: OBSERVATIONS

3.1. Identifying Clusters in Large Scale Surveys of Molecular Clouds

Unlike gravitationally bound open clusters or globular clusters, embedded clusters are not isolated objects. In most cases, molecular cloud complexes contain multiple embedded clusters as well as distributed populations of relatively isolated stars. Recent large scale surveys and all sky catalogs are now providing new opportunities to study the properties of embedded clusters through surveys of entire molecular clouds. The advantage of studying clusters by surveying entire molecular clouds is twofold. First, the surveys provide an unbiased sample of both the distributed and clustered populations within a molecular cloud. Second, the surveys result in an unbiased measurement of the distribu-

tion of cluster properties within a single cloud or ensemble of clouds. For the remainder of this discussion, we will use the word “cluster” to denote embedded clusters of young stars. Most of these clusters will not form bound open clusters (*Lada and Lada*, 1995).

We now concentrate on two recent surveys for young stars in relatively nearby (<1 kpc) molecular clouds. *Carpenter* (2000) used the 2MASS 2nd incremental point source catalog to study the distribution of young stars in the Orion A, Orion B, Perseus and Monoceros R2 clouds. Since the 2nd incremental release did not cover the entire sky, only parts of the Orion B and Perseus clouds were studied. More recently, *Spitzer* has surveyed a number of molecular clouds. We discuss here new results from the *Spitzer* Orion Molecular Cloud Survey (*Megeath et al.*, 2006) and the Cores to Disks (c2d) Legacy program survey of the Ophiuchus Cloud (*Allen et al.*, 2006). We use these data to study the distribution of the number of cluster members, the cluster radius, and the stellar density in this small sample of clouds.

The advantage of using these two surveys is that they draw from different techniques to identify populations of young stellar objects. The analysis of the 2MASS data relies on star counting methods (Section 2.5), while the *Spitzer* analysis relies on identifying young stars with infrared-excesses from combined *Spitzer* and 2MASS photometry (Section 2.1; *Megeath et al.* 2006). The 2MASS analysis is limited by the systematic and random noise from the background star subtraction, making the identification of small groups and distributed stars subject to large uncertainties. The *Spitzer* analysis is limited to young stars with disks or envelopes. A significant number of young stars in embedded clusters do not show excesses; this fraction may range from 20% to as much as 50% for 1-3 Myr clusters (*Haisch et al.*, 2001).

Carpenter (2000) identified stellar density peaks more than six times the RMS background noise, and defined a cluster as all stars in a closed 2σ contour surrounding these peaks. *Megeath et al.* (2006) defined clusters as groups of 10 or more IR-excess sources in which each member is within a projected distance of 0.32 pc of another member (corresponding to a density of 10 stars pc^{-2}). Only groups of ten or more neighbors are considered clusters. The clusters identified in the *Spitzer* survey are shown in Fig. 4.

3.2. The Fraction of Stars in Large Clusters

It is now generally accepted that most stars form in clusters (*Lada and Lada*, 1995), but quantitative estimates of the fraction of stars which form in large clusters, small clusters, groups and relative isolation are still uncertain. *Porras et al.* (2003) compiled a list of all known groups and clusters with more than 5 members within 1 kpc of the Sun, while *Lada and Lada* (2003) compiled the properties of a sample of 76 clusters with more than 36 members within 2 kpc. Although these compilations are not complete, they probably give a representative sample of clusters in the

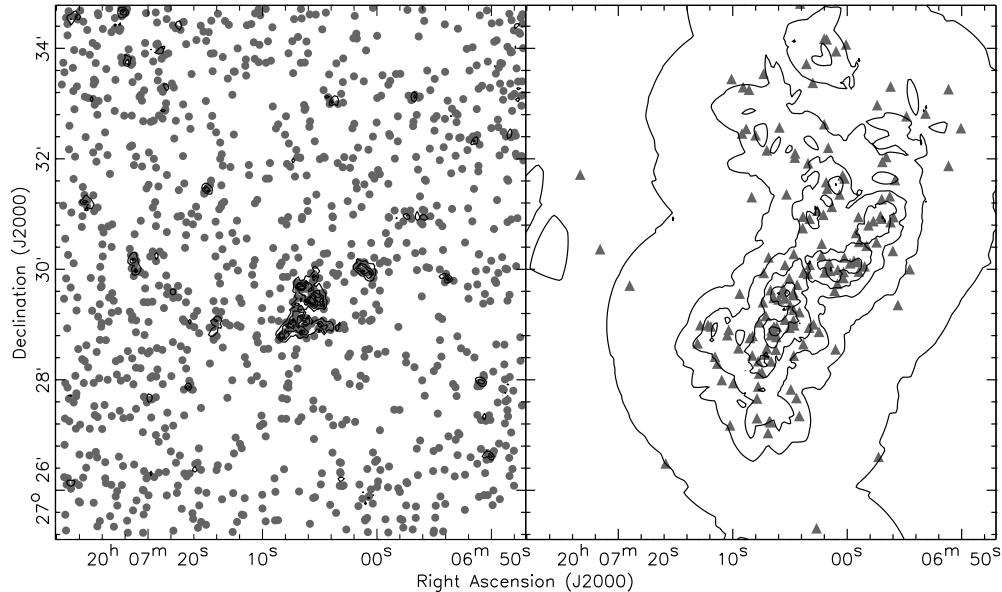


Fig. 3.— IRAS 20050 surface densities derived from the statistical technique applied to all stars (left), and from identifying the infrared-excess sources (right). In the left panel, all sources having $K < 16$ are plotted as a function of their position. Contours show the surface density of K-band sources, starting at 1450 pc^{-2} (5σ above median field star density) and increasing at intervals of 750 pc^{-2} . In the right panel, sources with infrared excess emission are plotted, and contours of their surface density are shown for 10, 60, 160, 360, 760, and 1560 pc^{-2} . The statistical technique (left) yields a higher peak surface density ($\sim 6000 \text{ pc}^{-2}$ at the center) than the IR-excess technique ($\sim 3000 \text{ pc}^{-2}$), but the latter is more sensitive to the spatially extended population of young stars.

nearest 1-2 kpc. In the sample of *Porras et al.* (2003), 80% of the stars are found in clusters with $N_{\text{star}} \geq 100$, and the more numerous groups and small clusters contain only a small fraction of the stars (also see *Lada and Lada*, 2003).

In Fig. 5, we plot the fraction of members from the 2MASS and *Spitzer* surveys as a function of the number of cluster size. Following the work of *Porras et al.* (2003), we divide the distribution into four sizes: $N_{\text{star}} \geq 100$, $100 > N_{\text{star}} \geq 30$, $30 > N_{\text{star}} \geq 10$, and $N_{\text{star}} < 10$. The main difference from the previous work is that we include a bin for $N_{\text{star}} < 10$; these we refer to as the distributed population. All of the observed molecular clouds appear to contain a distributed population. *Carpenter* (2000) estimated that the fraction of stars in the distributed population were 0%, 20%, 27%, and 44% for the Orion B, Perseus, Orion A and Mon R2 cloud, respectively, although the estimated fraction ranged from 0-66%, 13-41%, 0-61% and 26-59%, depending on the assumptions made in the background star subtraction. In the combined *Spitzer* survey sample, the fraction of distributed stars is 32-11%, 26-24%, and 25-21% for the Ophiuchus, Orion A and Orion B clouds respectively. The uncertainty is due to contamination from AGN: the higher fraction assumes no contamination, the lower number assumes that the distributed population contains 10 AGN for every square degree of map size. The

actual value will be in between those; extinction from the cloud will lower the density of AGN, and some of the contaminating AGN will be found toward clusters. In total, these measurements suggest that typically 20-25% of the stars are in the distributed population.

There are several caveats with this analysis. The first is the lack of completeness in the existing surveys. *Carpenter* (2000) considered the values of N_{star} as lower limits due to incompleteness and due to the masking of parts of the clusters to avoid artifacts from bright sources. Completeness is also an issue in the center of the Orion Nebula Cluster (ONC) for the *Spitzer* measurements. Also, we have not corrected the *Spitzer* data for the fraction of stars which do not show infrared excesses, the actual number of stars may be as much as a factor of two higher (*Gutermuth et al.*, 2004).

Another uncertainty is in the definition of the clusters. The clusters identified by these two methods are not entirely consistent. For example, in Orion A there is an uncertainty in the boundaries of the ONC. There is a large halo of stars surrounding this cluster, and the fraction of young stars in large clusters is dependent on whether stars are grouped in the ONC, in nearby smaller groups, or the distributed population. Both the 2MASS and the *Spitzer* data lead to an expansive definition of this cluster, extending

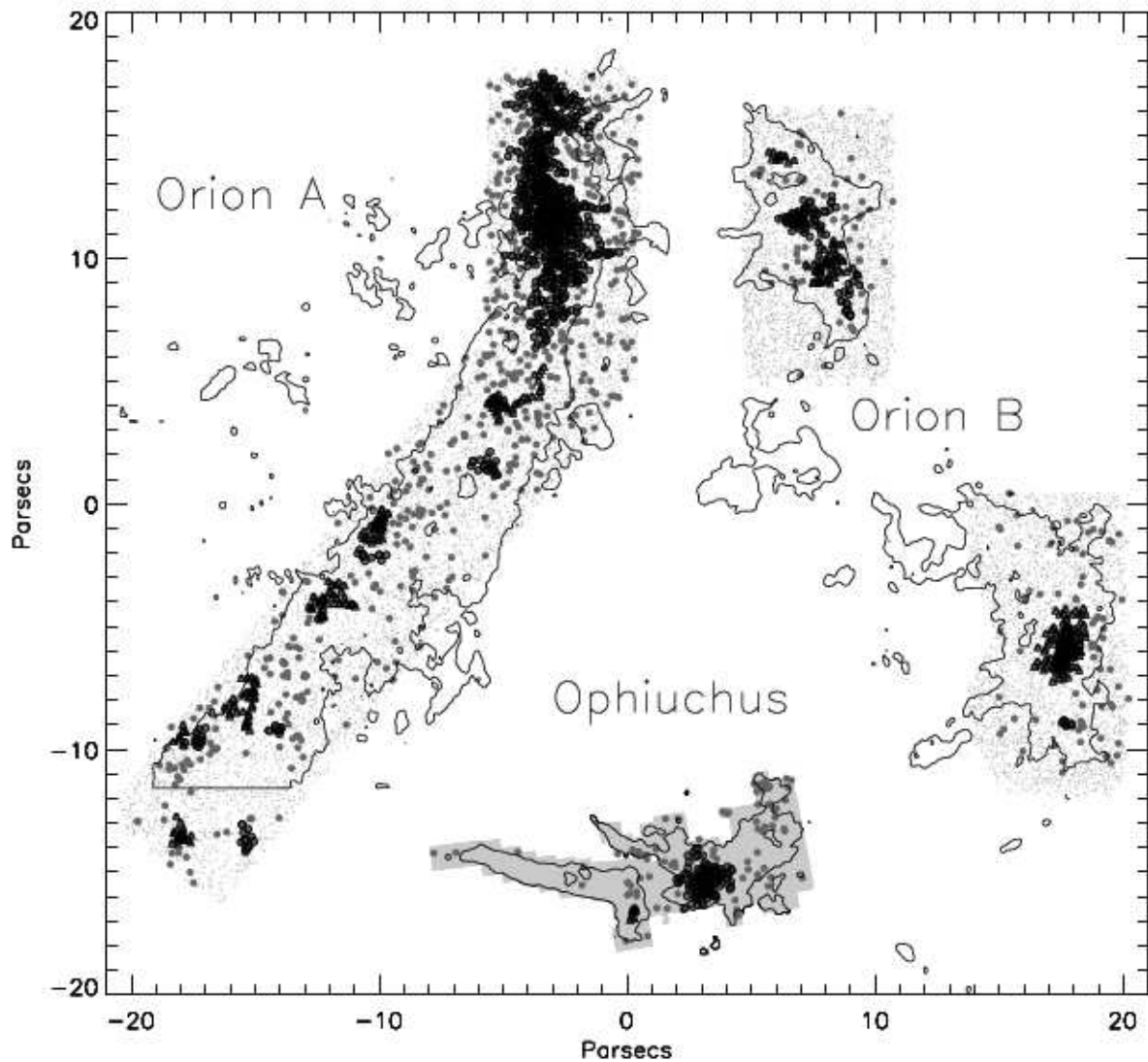


Fig. 4.— The spatial distribution of all Spitzer identified infrared excess sources from the combined IRAC and 2MASS photometry of Orion A (left), Orion B (right) and Ophiuchus (bottom center). The contours outline the Bell Labs ^{13}CO maps for the Orion A and B clouds (Bally *et al.*, 1987; Miesch and Bally, 1994), and an A_V map of Ophiuchus (Huard, 2006). The small grey dots show all the detections in the Spitzer 3.6 and 4.5 μm bands with magnitudes brighter than 15th and uncertainties less than 0.15. The large grey dots are the sources with infrared excesses. The black circles and triangles are sources found in clusters using the method described in Section 3.1; the two symbols are alternated so that neighboring clusters can be differentiated. Note that there are two clusters in the Orion A cloud which are below the lower boundary of the Bell Labs map. Each of the clouds has a significant distributed population of IR-excess sources.

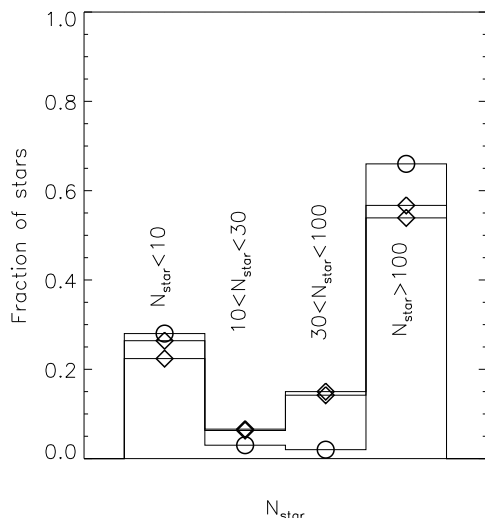


Fig. 5.— The distribution of the fraction of stars in clusters taken from *Carpenter* (2000) (circles) and the *Spitzer* surveys of Orion and Ophiuchus (diamonds). The *Spitzer* surveys show a range, depending on whether corrections are made for background AGN. In both the 2MASS and *Spitzer* surveys, the distributed population ($N_{star} < 10$) accounts for more than 20% of the total number of stars.

beyond the Orion Nebula and incorporating the OMC2/3 and NGC 1977 regions, as well the L1641 North group for the 2MASS analysis. The resulting cluster contains a significant number of stars in a relatively low stellar density environment far from the O-stars exciting in the nebula, which differs significantly from the environment of the dense core of the cluster embedded in the Orion Nebula. The treatment of the ONC is critical to this analysis: 50% (for the 2MASS sample) to 76% (for the *Spitzer* sample) of the stars in large clusters ($N_{star} \geq 100$) are found in the ONC.

A final caveat is that these results apply to the current epoch of star formation in the nearest kiloparsec. While the largest cluster within 1 kpc is the ONC with 1000-2000 members, a growing number of young super star clusters, which contain many thousands of stars, have been detected in our Galaxy. Super star clusters may bridge the gap between embedded clusters in the nearest kiloparsec, and the progenitors of the globular clusters which formed earlier in our Galaxy's history. Thus, the distribution of cluster sizes we have derived may not be representative for other regions of the Galaxy, or early epochs in our Galaxy's evolution.

3.3. The Surface Density of Stars in Embedded Clusters

In a recent paper, *Adams et al.* (2006) found a correlation between the number of stars in a cluster and the radius of the cluster, using the tabulated cluster properties in *Lada and Lada* (2003). They found that the correlation is even stronger if only the 2MASS identified clusters from

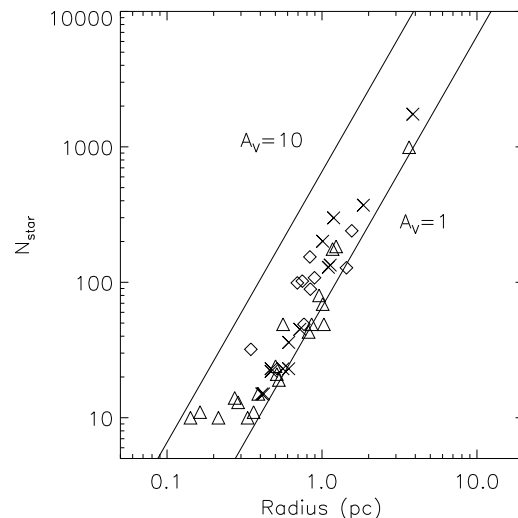


Fig. 6.— N_{star} vs. cluster radius for the 2MASS survey (crosses) of *Carpenter* (2000), the *Spitzer* Ophiuchus and Orion surveys (triangles) of *Megeath et al.* (2006) and *Allen et al.* (2006), and the *Spitzer* young stellar cluster survey (diamonds). Lines of constant column density are shown for a column density for $A_V = 1$ and $A_V = 10$. The average surface density of cluster members varies by less than an order of magnitude.

Carpenter (2000) were used, in which case the parameters were derived in a uniform manner. The same correlation is seen in a sample of clusters defined by *Spitzer* identified IR-excess sources. This correlation is shown for the 2MASS and *Spitzer* samples in Fig. 6. This relationship shows that while N_{star} varies over 2 orders of magnitude and the cluster radius ($R_{cluster}$) varies by almost 2 orders of magnitude, the average surface density of cluster members ($N_{star}/\pi R_{cluster}^2$) varies by less than one order of magnitude. The lower surface ($A_V = 1$) envelope of this correlation may result in part from the methods used to identify clusters. In particular, for the many clusters surrounded by large, low surface density halos of stars, the measured radius and density of these clusters depends on the threshold surface density or spatial separation used to distinguish the cluster stars from those in the halos. We can convert the surface densities of members into column densities of mass by assuming an average stellar mass of $0.5 M_{\odot}$. Assuming a standard abundance of hydrogen, and the typical conversion from hydrogen column density to A_V , we plot lines of constant A_V in Fig. 6. In this figure the clusters are bracketed by lines equivalent to $A_V \sim 1$ and $A_V \sim 10$. Interestingly, this result is similar to one of *Larson's* laws for molecular clouds, that the average column density of gas in molecular clouds is independent of cloud size and mass (*Larson*, 1985; see also the chapter by *Blitz et al.*).

3.4. The Spatial Structure of Embedded Clusters

One of the major goals of the *Spitzer* young stellar cluster and Orion surveys is to systematically survey the range of cluster morphologies by identifying the young stellar objects with disks and envelopes in these clusters. An initial result of this effort is displayed for ten clusters in Fig. 7, which shows the surface density of IR-excess sources. In this section, we give a brief overview of the common structures found in embedded clusters, both in the literature and in the sample of clusters imaged with *Spitzer*. We also discuss *ISO* and *Spitzer* observations of the youngest objects in these regions, the Class I and 0 sources.

Many of the clusters shown in Fig. 7 appear elongated; this had also been evident in some of the earlier studies of clusters (Carpenter *et al.*, 1997; Hillenbrand and Hartmann, 1998). To quantify this asymmetry, Gutermuth *et al.* (2005, 2006) compared the distribution of stars as a function of position angle to Monte Carlo simulations of circularly symmetric clusters, and demonstrated that the elongation is statistically significant in three of the six clusters in their sample. The elongation appears to be a result of the primordial structure in the cloud; for the two elongated clusters which have 850 μm dust continuum maps, the elongation of the cluster is aligned with filamentary structure seen in the parental molecular cloud. This suggests that the elongation results from the formation of the clusters in highly elongated, or filamentary, molecular clouds.

Not all clusters are elongated. Gutermuth *et al.* (2005) found no significant elongation of the NGC 7129 cluster, a region which also showed a significantly lower mean and peak stellar surface density than the more elongated clusters in his sample. Since the cluster was also centered in a cavity in the molecular cloud (see Section 5); they proposed that the lack of elongation was due to the expansion of the cluster following the dissipation of the molecular gas. However not all circularly symmetric clusters are easily explained by expansion; Gutermuth *et al.* (2006) find two deeply embedded clusters with no significant elongation or clumps, but no sign of the gas dispersal evident in NGC 7129. These two clusters, Cepheus A and AFGL 490, show azimuthal symmetry, which may reflect the primordial structure of the cluster.

Examination of Fig. 7 reveals another common structure: low density halos surrounding the dense centers, or cores, of the clusters. With the exception of AFGL 490 and perhaps Cepheus A, all of the clusters in Fig. 7 show cores and halos. The core-halo structure of clusters has been studied quantitatively through azimuthally smoothed radial density profiles (Muench *et al.* 2003). Although these density profiles can be fit by power laws, King models, or exponential functions (Hillenbrand and Hartmann, 1998; Lada and Lada, 1995; Horner *et al.*, 1997; Gutermuth, 2005), the resulting fits and their physical implications can be misleading. As pointed out by Hartmann (2004), azimuthally averaged density profiles can be significantly steepened by elongation (Hartmann (2004) argues this for molecular cores,

but the same argument applies to clusters). A more sophisticated treatment is required to study the density profiles of elongated clusters.

It has long been noted that young stellar clusters are sometimes composed of multiple sub-clusters (Lada *et al.*, 1996; Chen *et al.*, 1997; Megeath *et al.*, 1996; Allen *et al.*, 2002; Testi, 2002). Clusters with multiple density peaks or sub-clusters were classified as hierarchical clusters by Lada and Lada (2003). In some cases it is difficult to distinguish between two individual clusters and sub-clusters within a single cluster. An example are the NGC 2068 and NGC 2071 clusters in the Orion B cloud (Fig. 4). These appear as two peaks in a more extended distribution of stars, although the cluster identification method described in Section 3.1 separated the two peaks into two neighboring clusters. In the sample of Gutermuth *et al.* (2005, 2006), clumpy structure was most apparent in the IRAS 20050 cluster (also see Chen *et al.*, 1997). In this cluster, the sub-clusters are associated with distinct clumps in the 850 μm map of the associated molecular cloud. This suggests that like elongation, sub-clusters result from structures in the parental molecular cloud.

3.5. The Distribution of Protostars

If the observed morphologies of embedded clusters result from the filamentary and clumpy nature of the parental molecular clouds, then the younger Class 0/I objects, which have had the least time to move away from their star formation sites, should show more pronounced structures than the older, pre-main sequence Class II and Class III stars. Lada *et al.* (2000) found a deeply embedded population of young stellar objects with large $K - L$ colors toward the ONC; these protostar candidates showed a much more elongated and clumpy structure than the young pre-main sequence stars in the Orion Nebula. Using the methods described in Section 2.1, we have identified Class 0/I and II objects in clusters using combined *Spitzer* and ground-based near-IR photometry. In Fig. 8, we plot the distribution of class 0/I and II sources for four clusters in our sample. In the L1688 and IRAS 20050 clusters, the protostars fall preferentially in small sub-clusters, and are less widely distributed than the Class II objects. In the Serpens and GGD 12-15 clusters, the protostars are organized into highly elongated distributions. An interesting example containing multiple elongated distributions of protostars is the "spokes" cluster of NGC 2264, which shows several linear chains of protostars extending from a bright infrared source (Teixeira *et al.*, 2006). These chains, which give the impression of spokes on a wheel, follow filamentary structures in the molecular cloud. These data support the view that the elongation and sub-clustering are indeed the result of the primordial distribution of the parental dense gas. It is less clear whether the observed halos result from dynamical evolution or originate *in situ* in less active regions of star formation surrounding the more active cluster cores. The current data suggest that the halos are at least in part primordial; class 0/I objects are

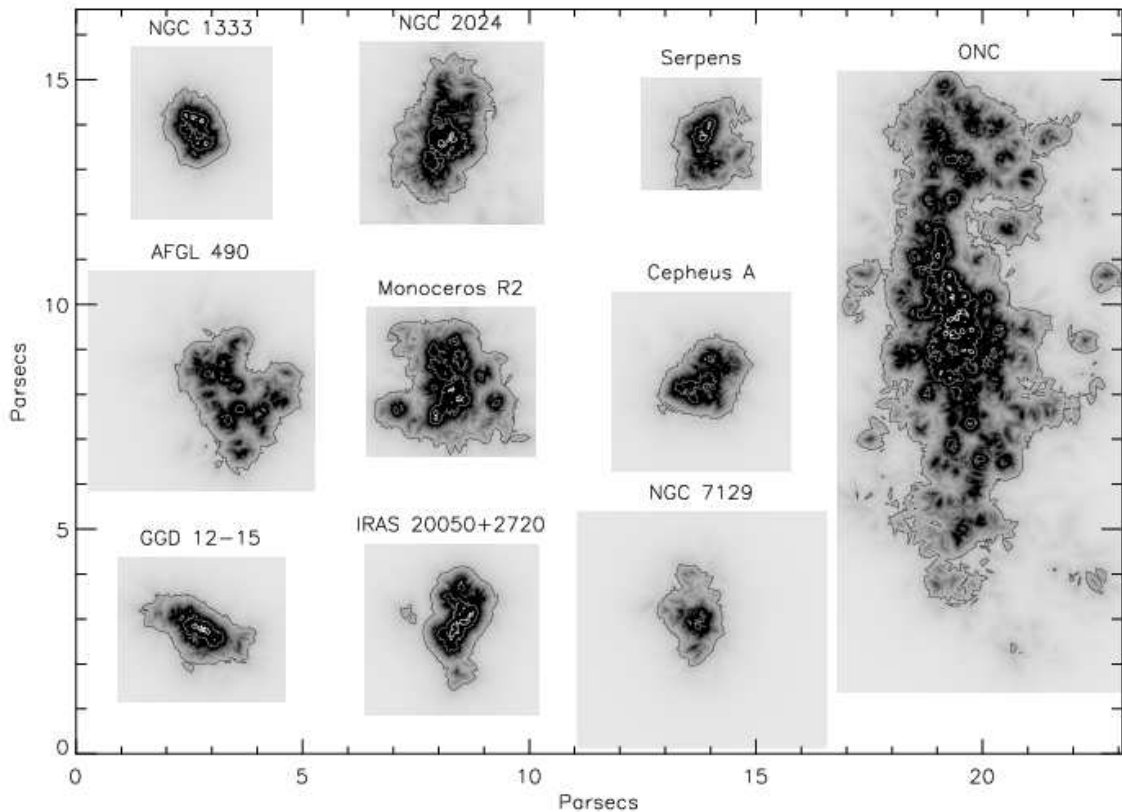


Fig. 7.— The distribution of infrared excess sources in ten clusters surveyed with *Spitzer*. The contours are at 1, 10 and 100 IR-excess sources pc^{-2} . These data clearly show that clusters are not circularly symmetric, but are often elongated. Some of the clusters, such as IRAS 20050, show distinct clumpy structure, although much of the small scale structure seen in the highest contours is due to statistical fluctuations in the smoothing scale. The three most circularly symmetric clusters are Cepheus A, AFGL 490 and NGC 7129; the irregular structure in these clusters is due in part to statistical fluctuations in regions of lower surface density.

observed in the halos of many clusters (*Gutermuth et al.*, 2004; *Megeath et al.*, 2004).

The spacing of protostars is an important constraint on the physical mechanisms for fragmentation and possible subsequent interactions by protostars. *Kaas et al.* (2004) analyzed the spacing of Class I and II objects identified in *ISO* imaging of the Serpens cluster. They calculated the separations of pairs of Class I objects, and found that the distribution of these separations peaked at 0.12 pc. In comparison, the distribution of separations for Class II objects show only a broad peak at 0.2 to 0.6 pc; this reflects the more spatially confined distributions of protostars discussed in the previous section. *Teixeira et al.* (2006) performed a similar analysis for the sample of protostars identified in the spokes cluster of NGC 2264. The distribution of nearest neighbor separations for this sample peaked at 0.085 pc; this spacing is similar to the Jeans length calculated from observations of the surrounding molecular gas.

Although the observed typical spacing of protostars in Serpens and NGC 2264 appears to be ~ 0.1 pc, as shown in Fig. 8, dense groups of protostars are observed in both these

regions (and others) in which several Class I/0 sources are found within a region 0.1 pc in diameter. This is the distance a protostar could move in 100,000 years (the nominal protostellar lifetime) at a velocity of 1 km s^{-1} . This suggests that if the velocity dispersion of protostars is comparable to the turbulent velocity dispersion observed in molecular clouds, interactions between protostars may occur, particularly in dense groupings. On the other hand, observations of some dense star-forming clumps show motions through their envelopes much less than 1 km s^{-1} (*Walsh et al.* 2004). The densest grouping of protostars so far identified in the *Spitzer* survey is found in the spokes cluster. One of the protostars in the spokes has been resolved into a small system of 10 protostars by ground-based near-IR imaging and by *Spitzer* IRAC imaging. These protostars are found in a region 10,000 AU in diameter. It is not clear whether these objects are in a bound system, facilitating interactions as the sources orbit within the system, or whether the stars are drifting apart as the molecular gas binding the region is dispersed by the evident outflows (*Young et al.*, 2006). It should be noted that this group of 10 protostars

appears to be the only such system in the spokes cluster. Thus, although dense groups of protostars are present in star forming regions, they may not be common.

4. GAS DISRUPTION AND THE LIFETIME OF EMBEDDED CLUSTERS

In the current picture of cluster evolution, star formation is terminated when the parental gas has dispersed. An understanding of the mechanisms and time scales for the disruption of the gas is necessary for understanding the duration of star formation in clusters, the lifetime and eventual fate of the clusters, and the ultimate star formation efficiency achieved in a molecular cloud.

The most massive stars have a disproportionate effect on cluster evolution. Massive O stars can rapidly disrupt the parental molecular cloud through their ionizing radiation. The effect of the disruption is not immediate; once massive stars form in a molecular core, star formation may continue in the cluster while the massive star remains embedded in an ultracompact HII region. Examples of clusters in this state within 1 kpc of the Sun are the GGD 12-15 and Mon R2 clusters. The timescale for the disruption of the core is equivalent to the lifetime of the ultracompact HII region (*Megeath et al.*, 2002); this lifetime is thought to be $\sim 10,000$ years for the solar neighborhood (*Casussus et al.*, 2000; *Comeron and Torra*, 1996).

In our sample of nearby embedded clusters, most systems do not contain O-stars. However, a number of partially embedded clusters in the nearest 1 kpc show evidence for significant disruption by B type stars. Due to the partial disruption of the clouds, the clusters in these regions are found in cavities filled with emission from UV heated polycyclic aromatic hydrocarbons (*Gutermuth et al.*, 2004). The time scale for the disruption by B stars can be estimated using measurements of the ages of the clusters. In our survey of nearby regions, we have three examples of regions with such cavities: NGC 7129 (earliest member B2), IC 348 (earliest member B5) and IC5146 (earliest member B0-1), with ages 2 Myr, 3 Myr and 1 Myr, respectively (*Hillenbrand et al.*, 1992; *Hillenbrand*, 1995; *Luhman et al.*, 2003; *Herbig and Dahm*, 2002). The presence of large, UV illuminated cavities in these regions suggest that the non-ionizing far-ultraviolet radiation (FUV) from B-stars may be effective at heating and evaporating molecular cloud surfaces in cases where intense FUV radiation from O-stars is not present. For example, in the case of NGC 7129, *Morris et al.* (2004) find that the temperature at the molecular cloud surface has been heated to 700 K by the FUV radiation. Future work is needed to determine if the high temperatures created by the FUV radiation can lead to substantial evaporative flows.

In regions without OB stars, however, some other mechanism must operate. An example is IRAS 20050. Based on SCUBA maps, as well as the reddening of the members, *Gutermuth et al.* (2005) found that the cluster is partially offset from the associated molecular gas, suggesting that

the gas had been partially dispersed by the young stars. Although this region contains no OB stars, it displays multiple outflows (*Chen et al.* 1997). Another example may be the NGC 1333 cloud, where *Quillen et al.* (2005) found evidence of wind-blown cavities in the molecular gas. In these regions, outflows may be primarily responsible for dissipating the dense molecular gas (e.g., *Matzner and McKee* 2000).

It is important to note that star formation continues during the gas dissipation process. Even when the gas around the main cluster has been largely disrupted (such is the case in the ONC, IC 348 and NGC 7129), star formation continues on the outskirts of the cluster in regions where the gas which has not been removed. Thus, the duration of star formation in these regions appears similar to the gas dispersal time of $\sim 1 - 3$ Myr. Older clusters have not been found partially embedded in their molecular gas (*Leisawitz et al.*, 1989).

5. EARLY CLUSTER EVOLUTION

Theories of cluster formation are reviewed elsewhere in these proceedings (see the chapters by *Ballesteros-Paredes et al.* and *Bonnell et al.*). Here we will discuss the dynamical evolution of young clusters during the first few million years.

Although most stars seem to form within clusters of some type (see Section 4), only about ten percent of stars are born within star-forming units that are destined to become open clusters. As a result, for perhaps 90 percent of forming stars, the destruction of their birth aggregates is an important issue. Star formation in these systems is not 100 percent efficient, so a great deal of cluster gas remains in the system. This gaseous component leaves the system in a relatively short time (a few Myr – see above) and its departure acts to unbind the cluster. At the zeroth level of understanding, if the star formation efficiency (SFE) is less than 50%, then a substantial amount of unbinding occurs when gas is removed. However, this description is overly simple. The stars in the system will always have a distribution of velocities. When gas is removed, stars on the high velocity tail of the distribution will always leave the system (even for very high SFE) and those on the extreme low velocity tail will tend to stay (even for low SFE). The fraction of stars that remain bound after gas removal is thus a smooth function of star formation efficiency (several authors have tried to calculate the function: see *Adams*, 2000; *Boily and Kroupa*, 2003a, 2003b; *Lada et al.*, 1984). The exact form of the bound fraction, $f_b(\epsilon)$, which is a function of SFE, depends on many other cluster properties: gas removal rates, concentration of the cluster, total depth of the cluster potential well, the distribution functions for the stellar velocities (radial vs isotropic), and the spatial profiles of the gaseous and stellar components (essentially, the SFE as a function of radial position). At the crudest level, the bound fraction function has the form $f_b \approx \sqrt{\epsilon}$, but the aforementioned complications allow for a range of forms.

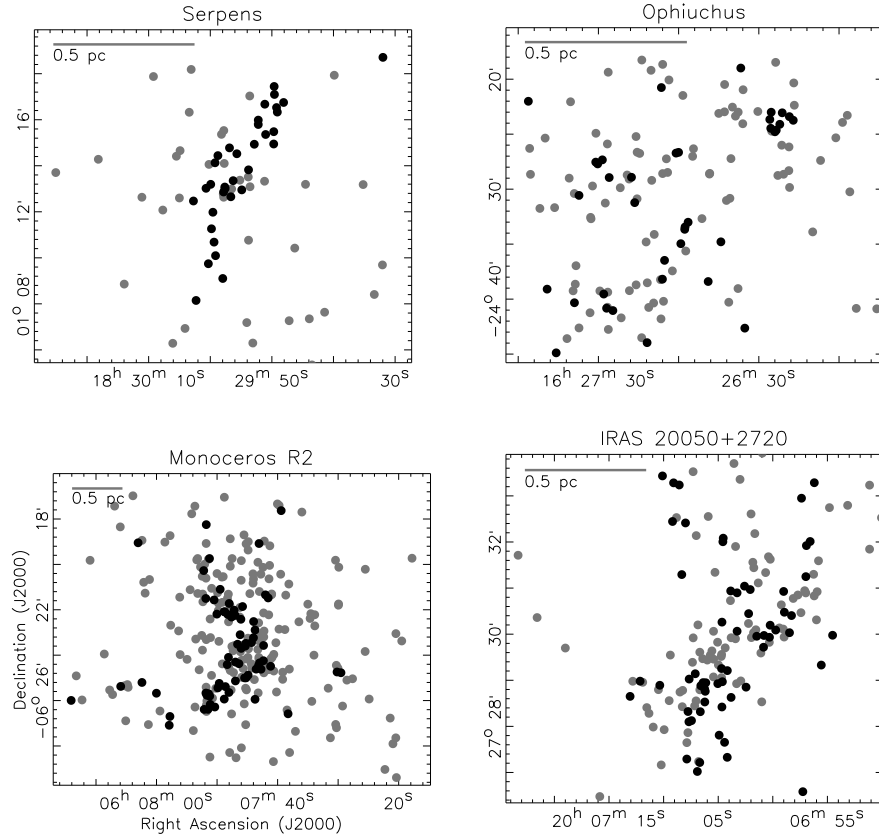


Fig. 8.— The spatial distributions of *Spitzer* identified class I/0 (dark circles) and Class II (light circles) objects in four clusters: L1688 in Ophiuchus, Serpens, Mon R2 and IRAS 20050. The Class I/0 sources are often distributed along filamentary structures, while the Class II sources are more widely distributed. Many small groups of protostars are dense enough that interactions between individual objects may occur.

The manner in which a cluster spreads out and dissolves after its gas is removed is another important problem. After gas removal, clusters are expected to retain some stars as described above, but such systems are relatively short-lived. For example, consider a cluster with $N = 100$ in its early embedded phase, before gas removal. After the gas leaves, typically one half to two thirds of the stars will become unbound along with the gas. The part of the cluster that remains bound will thus contain only $N = 30 - 50$ stars. Small groups with $N < 36$ have relaxation times that are shorter than their crossing times (Adams, 2000) and such small units will exhibit different dynamical behavior than their larger counterparts. In particular, such systems will relax quickly and will not remain visible as clusters for very long.

As more data are taken, another mismatch between theory and observations seems to be emerging: The theoretical calculations described above start with an established cluster with a well-defined velocity distribution function, and then remove the gaseous component and follow the evolution. Given the constant column density relationship for clusters (section 3.4), that the velocity of the stars are viri-

alized, and assuming that 30% of the cluster mass is in stars (see Lada and Lada, 2003), then the crossing time for the typical cluster in our sample is ~ 1 Myr (although it can be shorter in the dense centers of clusters). As a result, in rough terms, the gas removal time, the duration of star formation, and the crossing time are comparable. This implies that partially embedded clusters may not have enough time to form relaxed, virial clusters; this in turn may explain in part the range of morphologies discussed in Section 3.

6. EFFECTS OF CLUSTERS ON STAR AND PLANET FORMATION

The radiation fields produced by the cluster environment can have an important impact on stars and planets formed within. Both the extreme, ionizing UV (EUV) and the far-UV (FUV) radiation can drive disk evaporation (Shu *et al.*, 1993; Johnstone *et al.*, 1998; Störzer and Hollenbach, 1999; Armitage, 2000). In the modest sized clusters of interest here (100-1000 stars), the mass loss driven by FUV radiation generally dominates (e.g., Adams *et al.*, 2004), although EUV photoevaporation can also be important (Armitage, 2000; Johnstone *et al.*, 1998; Shu *et al.*,

1993; Störzer and Hollenbach, 1999). For clusters with typical cluster membership e.g., with $N_{star} = 300$ (Section 3.1), the average solar system is exposed to a FUV flux of $G \approx 1000 - 3000$ (Adams et al., 2006), where $G = 1$ corresponds to a flux of $1.6 \times 10^{-3} \text{ erg cm}^{-2} \text{ s}^{-1}$. FUV fluxes of this magnitude will evaporate a disk orbiting a solar type star down to a truncation radius of about 50 AU over a time scale of 4 Myr. As a result, planet forming disks are relatively immune in the regions thought to be relevant for making giant gaseous planets. Forming solar systems around smaller stars are more easily evaporated for two reasons. First, the central potential well is less deep, so the stellar gravity holds less tightly onto the disk gas, which is more easily evaporated. Second, we expect the disk mass to scale linearly with stellar mass so that disks around smaller stars have a smaller supply and can be evaporated more quickly. With these disadvantages, M stars with $0.25 M_{\odot}$ can be evaporated down to 10 AU in 4 Myr with an FUV radiation field of $G = 3000$. In larger clusters with more massive stars, Adams et al. (2004) find that regions with strong FUV and EUV can affect disks around solar mass stars on solar system size scales, truncating an initially 100 AU disk to a radius of 30 AU in 4 Myr.

A full assesment of the importance of UV radiation on disks needs to be informed by the observed properties of clusters. What fraction of stars in the *Spitzer* and 2MASS samples are found in clusters with significant EUV radiation fields? We use the presence of an HII region as an indicator of a EUV field. In the *Spitzer* sample (the Orion A, Orion B and Ophiuchus clouds) the two clusters with HII regions contain 45% of the IR-excess sources. In the 2MASS sample (Orion A, Orion B, Perseus and Monoceros R2), 55% of the young stars are found in the four clusters with HII regions. Thus, a significant fraction of stars is found in clusters with HII regions. However, in both the 2MASS and *Spitzer* samples most of the stars found in clusters with HII regions are found in the ONC. The ONC has a radius of 4 pc and many of the low mass stars in this cluster are more than a parsec away from the massive stars, which are concentrated in the center of the cluster. Thus, the fraction of stars exposed to a significant EUV field appears to be less than 50%. However, a more systematic determination of this fraction should be made as data become available.

In addition to driving photoevaporation, EUV radiation (and X-rays) can help ionize the disk gas. This effect is potentially important. One of the most important mechanisms for producing disk viscosity is through magneto-rotational instability (MRI), and this instability depends on having a substantial ionization fraction in the disk. One problem with this idea is that the disk can become too cold and the ionization fraction can become too low to sustain the turbulence. If the background environment of the cluster provides enough EUV radiation, then the cluster environment can be important for helping drive disk accretion.

Clusters can also have an affect on the processes of star and planet formation through dynamical interactions. This raises a variant of the classic question of nature vs nurture:

are the properties of the protostars and the emergent stars influenced by interactions or are they primarily the result of initial conditions in a relatively isolated collapse? The numerical simulations of cloud collapse and cluster formation (Bate et al., 2003; Bonnell et al., 2003; Bonnell et al., 2004) predict that interactions are important, with the individual protostars competitively accreting gas from a common reservoir as they move through the cloud, and dynamical interactions between protostars resulting in ejections from the cloud.

We assess the importance of interactions given our current understanding of cluster structure. The density of clusters, and of protostars in clusters, suggest that if stars move with velocities similar to the turbulent gas velocity ($\sim 1 \text{ kms}^{-1}$), interactions can occur in the lifetime of a protostar (100,000 yr). Gutermuth et al. (2005) found typical stellar densities of $10^4 \text{ stars pc}^{-3}$ in the cores of two young clusters. If the velocity dispersion is 1 kms^{-1} , most protostars will pass within 1000 AU - the size of a protostellar envelope - of another star or protostars within a protostellar lifetime. The observed spacing of Class I/0 sources discussed in Section 3.2 also suggests that interactions can occur in some cases. At these distances protostars could compete for gas or interact through collisions of their envelopes. Interestingly, recent data suggest that, at least in some clusters, the observed pre-stellar clumps that make up the initial states for star formation are not moving dynamically, but rather have subvirial velocities (Walsh et al., 2004; Peretto et al., 2006). If these clusters are typical, then interactions between protostars in clusters would be minimal.

Given the observed surface densities of clusters, is it possible that a cluster could result from the collapse of individual, non-interacting pre-stellar cores (i.e. nature over nurture)? If the starting density profile of an individual star formation event can be modeled as an isothermal sphere, then its radial size would be given by $r = GM_*/2a^2 \approx 0.03 \text{ pc}$ (where we use a typical stellar mass of $M_* = 0.5 M_{\odot}$ and sound speed $a = 0.2 \text{ kms}^{-1}$). A spherical volume of radius $R = 1 \text{ pc}$ can thus hold about 37,000 of these smaller spheres (in a close-packed configuration). Thus, we can conclude that there is no *a priori* geometrical requirement for the individual star forming units to interact.

Once a star sheds or accretes its protostellar envelope, direct collisions are relatively rare because their cross sections are small. Other interactions are much more likely to occur because they have larger cross sections. For example, the disks around newly formed stars can interact with each other or with passing binaries and be truncated (Kobayashi and Ida, 2001; Ostriker, 1994). In rough terms, these studies indicate that a passing star can truncate a circumstellar disk down to a radius r_d that is one third of the impact parameter. In addition, newly formed planetary systems can interact with each other, and with passing binary star systems, and change the planetary orbits (Adams and Laughlin, 2001). In a similar vein, binaries and single stars can interact with each other, exchange partners, form new binaries, and/or ionize existing binaries (McMillan and Hut,

1996; *Rasio et al.*, 1995).

To affect a disk on a solar system (40 AU) scale requires a close approach at a distance of 100 AU or less. *Gutermuth et al.* (2005) estimated the rate of such approaches for the dense cores of clusters. They estimate that for the typical density of 10^4 stars per pc^{-3} , the interaction time is 10^7 years, longer than the lifetime of the cluster. For N-body models of the modest sized clusters of interest here (100-1000 members), the typical star/disk system is expected to experience about one close encounter within 1000 AU over the next ~ 5 Myr while the cluster remains intact; close encounters within 100 AU are rare (e.g., *Adams et al.*, 2006; *Smith and Bonnell*, 2001). Given that lifetime of the cluster is less than 5 Myr, these models again indicate a minimal effect on nascent solar systems.

7. CONCLUSIONS

1. The Distribution of Cluster Properties: Systematic surveys of giant molecular clouds from 2MASS and *Spitzer*, as well as targeted surveys of individual clusters, are providing the first measurements of the range and distribution of cluster properties in the nearest kiloparsec. Although most stars appear in groups or clusters, in many star-forming regions there is a significant distributed component. These results suggest that there is a continuum of star-forming environments from relative isolation to dense clusters. Theories of star formation must take into account (and eventually explain) this observed distribution. The 2MASS and *Spitzer* surveys also show a correlation between number of member stars and the radii of clusters, such that the average surface density of stars varies by a factor of only ~ 5 .

2. The Structure of Young Stellar Clusters: Common cluster morphologies include elongation, low density halos, and sub-clustering. The observed cluster and molecular gas morphologies are similar, especially when only the youngest Class I/O sources are considered. This similarity suggests that these morphologies (except possibly halos) result from the distribution of fragmentation sites in the parental cloud, and not the subsequent dynamical evolution of the cluster. Consequently, the surface densities and morphologies of clusters are important constraints on models of the birth of clusters.

3. The Evolution of Clusters: The evolution of clusters is driven initially by the formation of stars, and then later on by the dissipation of gas. Gas dissipation appears to be driven by different processes in different regions, including photoevaporation by extreme-UV from O stars, photoevaporation by far-UV radiation from B stars, and outflows from lower mass stars. Much of the gas appears to be dissipated in 3 Myr which is a few times the crossing time and the duration of star formation in these clusters. With these short timescales, clusters probably never reach dynamical equilibrium in the embedded phase. The survival of clusters as the gas is dispersed is primarily a function of the size of

the cluster, the efficiency of star formation, and the rate at which the gas is dispersed.

4. The Impact of Clustering on Star and Planet Formation: Far-UV and Extreme-UV radiation from massive stars can effectively truncate disks in a few million years. Extreme UV radiation is needed to affect disks around solar type stars on solar system scales (< 40 AU) in the lifetime of the cluster. Within our sample of molecular clouds, fewer than 50% of the stars are found in regions with strong extreme UV-fields. The observed spacing of protostars suggest that dynamical interactions and competitive accretion may occur in the denser regions of the observed clusters. However, evidence of sub-virial velocities of pre-stellar condensations in at least one cluster hints that these interactions may not be important. Given the densities and lifetimes of the observed clusters, dynamical interactions do not appear to be an important mechanism for truncating disks on solar system size scales.

ACKNOWLEDGMENTS This work is based in part on observations made with the *Spitzer Space Telescope*, which is operated by the Jet Propulsion Laboratory, California Institute of Technology under NASA contract 1407. Support for this work was provided by NASA through Contract Numbers 1256790 and 960785, issued by JPL/Caltech. PCM acknowledges a grant from the *Spitzer* Legacy Science Program to the “Cores to Disks” team and a grant from the NASA Origins of Solar Systems Program. S.J.W. received support from *Chandra* X-ray Center contract NAS8-39073. FCA is supported by NASA through the Terrestrial Planet Finder Mission (NNG04G190G) and the Astrophysics Theory Program (NNG04GK56G0).

REFERENCES

- Adams F. C. (2000) *Astrophys. J.*, 542, 964-973.
- Adams F. C. and Laughlin G. (2001) *Icarus*, 150, 151-162.
- Adams F. C., Lada C. J., and Shu F. H. (1987) *Astrophys. J.*, 312, 788-806.
- Adams F. C., Hollenbach D., Laughlin G., and Gorti U. (2004) *Astrophys. J.*, 611, 360-379.
- Adams F. C., Proszkow E. M., Fatuzzo M., and Myers P. C. (2006) *Astrophys. J.*, in press, astro-ph/0512330
- Allen L. E., Myers P. C., Di Francesco J., Mathieu R., Chen H., and Young E. (2002) *Astrophys. J.*, 566, 993-1004.
- Allen L. E., Calvet N., D'Alessio P., Merin B., Hartmann L., Megeath S. T., et al. (2004) *Astrophys. J. Suppl.*, 154, 363-366.
- Allen L. E., Hora J. L., Megeath S. T., Deutsch L. K., Fazio G. G., Chavarria L., and Dell R. D. (2005) *Massive Star Birth: A Crossroads of Astrophysics* (R. Cesaroni, E. Churchwell, M. Felli, and C. M. Walmsley eds.), pp. 352-357. Cambridge University Press, Cambridge.
- Allen L. E., Harvey P., Jorgensen J., Huard T., Evans N. J. II et al. (2006) in prep.
- André P., Ward-Thompson D., and Barsony M. (1993) *Astrophys. J.*, 406, 122-141.

- André P., Ward-Thompson D., and Barsony M. (2000) *Protostars and Protoplanets IV* (V. Mannings, A. Boss, S. Russell, eds.), pp. 59-96. University of Arizona, Tucson.
- Armitage P. J. (2000) *Astron. Astrophys.*, 362, 968-972.
- Bally, J., Stark A. A., Wilson R. W., and Langer W. D. (1987) *Astrophys. J.*, 312, L45-L49.
- Bate M. R., Bonnell I. A., and Bromm V. (2003) *Mon. Not. R. Astron. Soc.*, 339, 577-599.
- Boily C. M. and Kroupa P. (2003a) *Mon. Not. R. Astron. Soc.*, 338, 665-672.
- Boily C. M. and Kroupa P. (2003b) *Mon. Not. R. Astron. Soc.*, 338, 673-686.
- Bonnell I. A., Bate M., and Vine S. G. (2003) *Mon. Not. R. Astron. Soc.*, 343, 413-418.
- Bonnell I. A., Vine S. G., and Bate M. (2004) *Mon. Not. R. Astron. Soc.*, 349, 735-741.
- Cambrésy L., Petropoulou V., Kontizas M., and Kontizas E. (2006) *Astron. Astrophys.*, 445, 999-1003.
- Carpenter J. M., Meyer M. R., Dougados C., Strom S. E., and Hillenbrand L. A. (1997) *Astron. J.*, 114, 198-221.
- Carpenter J. M. (2000) *Astron. J.*, 120, 3139-3161.
- Carpenter J. M., Hillenbrand L. A., and Skrutskie M. F. (2001) *Astron. J.*, 121, 3160-3190.
- Carpenter J. M., Hillenbrand L. A., Skrutskie M. F., and Meyer M. R. (2002) *Astron. J.*, 124, 1001-1025.
- Casassus S., Bronfman L., May J., and Nyman L. A. (2000) *Astron. Astrophys.*, 358, 514-520.
- Chen H., Tafalla M., Greene T. P., Myers P. C., and Wilner D. J. (1997) *Astrophys. J.*, 475, 163-172.
- Cameron F. and Torra J. (1996) *Astron. Astrophys.*, 314, 776-784.
- Dorren J. D., Guedel M., and Guinan E. F. (1995) *Astrophys. J.*, 448, 431-436.
- Evans N. J. II, Allen L. E., Blake G. A., Boogert A. C. A., Bourke T. et al. (2003) *Publ. Astron. Soc. Pac.*, 115, 965-980.
- Feigelson E. D. and Montmerle T. (1999) *Ann. Rev. Astron. Astrophys.*, 37, 363-408.
- Feigelson E. D., Getman K., Townsley L., Garmire G., Preibisch T., Grosso N., Montmerle T., Muench A., and McCaughrean M. (2005) *Astrophys. J. Suppl.*, 160, 379-389.
- Flaccomio E., Damiani F., Micela G., Sciortino S., Harnden F. R., Murray S. S., and Wolk S. J. (2003) *Astrophys. J.*, 582, 398-409.
- Flaherty K., Pipher J. L., Megeath S. T., Winston E. A., Gutermuth R. A., and Muzerolle J. (2006) *in prep.*
- Gladwin P. P., Kitsionas S., Boffin H. M. J., and Whitworth A. P. (1999) *Mon. Not. R. Astron. Soc.*, 302, 305-313.
- Gomez M., Hartmann L., Kenyon S. J., and Hewett R. (1993) *Astron. J.*, 105, 1927-1937.
- Greene T. P., Wilking B. A., André, P., Young, E. T., and Lada C. J. (1994) *Astrophys. J.*, 434, 614-626.
- Gutermuth R. A. (2005) *Ph.D. thesis*, Univ. of Rochester.
- Gutermuth R. A., Megeath S. T., Muzerolle J., Allen L. E., Pipher J. L., Myers P. C., and Fazio G. G. (2004) *Astrophys. J. Suppl.*, 154, 374-378.
- Gutermuth R. A., Megeath S. T., Pipher J. L., Williams J. P., Allen L. E., Myers P. C., and Raines S. N. (2005) *Astrophys. J.*, 632, 397-420.
- Gutermuth R. A., Pipher J. L., Megeath S. T., Allen L. E., Myers P. C., et al. (2006) *in prep.*
- Haisch K. E., Lada E. A., and Lada C. J. (2001) *Astrophys. J.* 553, L153-L156.
- Hartmann L. (2004) In *Star Formation at High Angular Resolution* (M. Burton, R. Jayawardhana, T. Bourke, eds.), pp. 201-211. ASP Conf. Series, San Francisco.
- Hartmann L., Megeath S. T., Allen L., Luhman K., Calvet N. et al. (2005) *Astrophys. J.*, 629, 881-896.
- Herbig G. H. and Dahm S. E. (2002) *Astron. J.* 123, 304-327.
- Herbig G. H. and Bell K. R. (1998) *Lick Observatory Bulletin, Santa Cruz: Lick Observatory, 1995*, VizieR Online Data Catalog, 5073.
- Hillenbrand L. A. (1995) *Ph.D. Thesis, University of Massachusetts.*
- Hillenbrand L. A., Strom S. E., Vrba F. J., and Keene J. (1992) *Astrophys. J.*, 397, 613-643.
- Hillenbrand L. A., Massey P., Strom S. E., and Merrill K. M. (1993) *Astron. J.*, 106, 1906-1946.
- Hillenbrand L. A. and Hartmann L. (1998) *Astrophys. J.*, 492, 540.
- Horner D. J., Lada E. A., and Lada C. J. (1997) *Astron. J.* 113, 1788-1798.
- Huard T. (2006) *private communication.*
- Johnstone D., Hollenbach D. J., and Bally J. (1998) *Astrophys. J.*, 499, 758-776.
- Kaas A. A. (1999) *Astron. J.*, 118, 558-571.
- Kaas A. A., Olofsson G., Bontemps S., André P., Nordh L. et al. (2004) *Astron. Astrophys.* 421, 623-642.
- Kobayashi H. and Ida S. (2001) *Icarus*, 153, 416-429.
- Lada E. A., Evans N. J. II, Depoy D. L., and Gatley I. (1991) *Astrophys. J.*, 371, 171-182.
- Lada C. J. and Lada E. A. (1995) *Astron. J.*, 109, 1682-1696.
- Lada C. J., Alves J., and Lada E. A. (1996) *Astron. J.*, 1111, 1964-1976.
- Lada C. J., Muench A. A., Haisch K. E., Lada E. A., Alves J. F., Tollestrup E. V., and Willner S. P. (2000) *Astron. J.*, 120, 3162-3176.
- Lada C. J. and Lada E. A. (2003) *Ann. Rev. Astron. Astrophys.*, 41, 57-115.
- Lada C. J., Margulis M., and Dearborn D. (1984), *Astrophys. J.*, 285, 141-152.
- Larson R. B. (1985) *Mon. Not. R. Astron. Soc.*, 214, 379-398.
- Leisawitz D., Bash F. N., and Thaddeus P. (1989) *Astrophys. J. Suppl.*, 70, 731-812.
- Luhman K. L., Stauffer J. R., Muench A. A., Rieke G. H., Lada E. A., Bouvier J., and Lada C. J. (2003) *Astrophys. J.*, 593, 1093-1115.
- Matzner C. D. and McKee C. F. (2000) *Astrophys. J.*, 545, 364-378.
- McMillan S. L. W. and Hut P. (1996) *Astrophys. J.*, 467, 348-358.
- Megeath S. T., Herter T., Beichman C., Gautier N., Hester J. J., Rayner J., and Shupe D. (1996) *Astron. Astrophys.*, 307, 775-790.
- Megeath S. T. and Wilson T. L. (1997) *Astron. J.*, 114, 1106-1120.
- Megeath S. T., Biller B., Dame, T. M., Leass E., Whitaker R. S., and Wilson T. L. (2002) *Hot Star Workshop III: The Earliest Stages of MAssive Star Formation* (P. A. Crowther, ed.), pp. 257-265. ASP Conf. Series, San Francisco.
- Megeath S. T., Allen L. E., Gutermuth R. A., Pipher J. L., Myers P. C. et al. (2004) *Astrophys. J. Suppl.*, 154, 367-373.
- Megeath S. T., Flaherty K. M., Hora J., Allen L. E., Fazio G. G. et al. (2005) *Massive Star Birth: A Crossroads of Astrophysics* (R. Cesaroni, E. Churchwell, M. Felli, and C. M. Walmsley eds.), pp. 383-388. Cambridge University Press, Cambridge.
- Megeath S. T., Flaherty K., Gutermuth R., Hora J., Allen L. E. et al. (2006) *in prep.*
- Micela G., Sciortino S., Serio S., Vaiana G. S., Bookbinder J.,

- Golub L., Harnden F. R., and Rosner R. (1985) *Astrophys. J.*, 292, 172-180.
- Miesch M. S. and Bally J. (1994) *Astrophys. J.*, 429, 645-671.
- Morris P. W., Noriega-Crespo A., Marleau F. R., Teplitz H. I., Uchida K. I., and Armus L. (2004) *Astrophys. J. Suppl.*, 154, 339-343.
- Motte F., André P. and Neri R. (1998) *Astron. Astrophys.*, 336, 150-172.
- Motte F., André P., Ward-Thompson D., and Bontemps S. (2001) *Astron. Astrophys.*, 372, L41-L44.
- Muench A. A., Lada E. A., Lada C. J., Elston R. J., Alves J. F., Horrobin M., Huard T. H. et al. (2003) *Astron. J.*, 125, 2029-2049.
- Muzerolle J., Megeath S. T., Gutermuth R. A., Allen L. E., Pipher J. L. et al. (2004) *Astrophys. J. Suppl.*, 154, 379-384.
- Muzerolle J., Megeath S. T., Flaherty K., Allen L. E., Young E. T. et al. (2006) *in prep.*
- Myers P. C. and Ladd E. F. (1993) *Astrophys. J.*, 413, L47-L50.
- Nutter D. J., Ward-Thompson D., and André P. (2005) *Mon. Not. R. Astron. Soc.*, 357, 975-982.
- Ostriker E. C. (1994) *Astrophys. J.*, 424, 292-318.
- Peretto N., André P., and Belloche A. (2006) *Astron. Astrophys.*, 445, 879-998.
- Porras A., Christopher M., Allen L., Di Francesco J., Megeath S. T., and Myers P. C. (2003) *Astron. J.*, 126, 1916-1924.
- Quillen A. C., Thorndike S. L., Cunningham A., Frank A., Gutermuth R. A., Blackmann E. G., Pipher J. L., and Ridge N. (2005) *Astrophys. J.*, 632, 941-955.
- Rasio F. A., McMillan S., and Hut P. (1995) *Astrophys. J.*, 438, L33-L36.
- Rodríguez L. F., Anglada G., and Curiel S. (1999) *Astrophys. J. Suppl.*, 125, 427-438.
- Sandell G. and Knee L. B. G. (2001) *Astrophys. J.*, 546, L49-L52.
- Shu F. H., Johnstone D., and Hollenbach D. J. (1993) *Icarus*, 106, 92-101.
- Smith K. W. and Bonnell I. A. (2001) *Mon. Not. R. Astron. Soc.*, 322, L1-L4.
- Stern D., Eisenhardt P., Gorjian V., Kochanek C. S., and Caldwell N. (2005) *Astrophys. J.*, 631, 163-168.
- Störzer H. and Hollenbach D. (1999) *Astrophys. J.*, 515, 669-684.
- Teixeira P. S., Lada C. J., Young E. T., Marengo M., and Muench A., et al. (2006) *Astrophys. J.*, 636, L45-L48.
- Testi L. (2002) In *Modes of Star Formation and the Origin of Field Populations* (E. K. Grebel and W. Brandner, eds.), pp. 60-70.
- Walsh A. J., Myers P. C., and Burton M. G. (2004) *Astrophys. J.*, 614, 194-202.
- Walter F. M. and Barry D. C. (1991) *The Sun in Time*, 633-657.
- Whitney B. A., Wood K., Bjorkman J. E., and Cohen M. (2003) *Astrophys. J.*, 598, 1079-1099.
- Wilking B. A., Schwartz R. D., and Blackwell J. H. (1987) *Astron. J.*, 94, 106-110.
- Wilking B. A., Lada C. J., and Young E. T. (1989) *Astrophys. J.*, 340, 823-852.
- Wiramihardja S. D., Kogure T., Yoshida S., Ogura K., and Nakano M. (1989) *Planet. Astron. Soc. Pac.*, 41, 155-174.
- Wolk S. J., Spitzbart B.D., Bourke T.L., and Alves J. (2006) *Astron. J.*, *submitted*.
- Young E. T., Teixeira P., Lada C. J., Muzerolle J., Persson S. E. et al. (2006) *Astrophys. J.*, *in press*, astro-ph/0601300.